Experimental demonstration of a self-tracking 16-aperture receive telescope array for laser intersatellite communications

Andras Kalmar, Klaus H. Kudielka, Walter R. Leeb

Institut für Nachrichtentechnik und Hochfrequenztechnik,
Technische Universität Wien,
Gußhausstraße 25/389, A-1040 Wien, Austria

ABSTRACT

An adaptive receive telescope array with 16 apertures has been designed and breadboarded. With respect to size and performance, such a telescope array is well suited for use as receive antenna in a coherent interorbit laser link.

The laboratory demonstrator, designed to operate at a wavelength of $\lambda = 1.064\mu m$, is completely independent of any subsequent receiver and of the data modulation format employed. The telescope array is self-phasing, i.e. the main lobe of the antenna pattern automatically follows the direction of the incident wave. It thus performs non-mechanical fine tracking.

Our experimental setup comprises a subtelescope array and a digital control unit employing digital signal processors. Besides inertia-free tracking, the control unit also checks and, if necessary, restores parallel alignment of the subtelescope axes at regular intervals. Space-worthy concepts have been applied wherever possible, although experiments have been performed only in the laboratory. Automatic fine-tracking is achieved within a single subtelescope's field of view ($30\mu rad$) in the frequency range up to $730Hz$.

Keywords: optical phased array, adaptive optics, laser space communications, optical receive antenna, non-mechanical antenna tracking

1. INTRODUCTION

Synthesizing a large aperture by arranging identical antennas to form a planar array is a well established concept in the microwave regime. The major advantage of such arrays is that the antenna pattern can be formed by phase shifting the single element fields.

Since the telescope diameters envisaged for free-space optical communication terminals are in the range of $10 \ldots 30cm$,[1] the laser beams used have widths on the order of only a few microradian. Such extremely narrow antenna characteristics ask for a fine-pointing accuracy in the sub-microradian regime. Moreover, due to platform vibrations caused by spacecraft attitude jitter, the fine-pointing mechanism has to be provided at frequencies up to several hundred Hertz. Using a phased telescope array, such fine and agile antenna pointing may be accomplished by electronic means. The accuracy required for the mechanical pointing unit, which is still imperative for coarse pointing and initial acquisition, is thereby greatly reduced. In comparison to a single telescope of the same aperture diameter, a telescope array further offers:

- reduced size of optical elements,
- inherent modularity, therefore
- redundancy (i.e. graceful degradation instead of total breakdown in case of a subtelescope failure), and
- reduced overall size and mass (as the length of a diffraction limited telescope scales with its diameter).

Other author information: (Send correspondence to A.K.)
A.K.: E-mail: Andras.Kalmar@tuwien.ac.at; Telephone: ++43 1 58801-3530; Telefax ++43 1 5870583
K.H.K.: E-mail: Klaus.Kudielka@tuwien.ac.at
W.R.L.: E-mail: Walter.Leeb@tuwien.ac.at

However, these advantages do not come without additional complexity compared to conventional approaches. First, one has to provide for a defined phase relationship between the individual subaperture fields. Considering the required pointing accuracy, it becomes clear that an active phase control mechanism with a resolution of a fraction of the wavelength has to be implemented. Second, the subtelescope axes have to be aligned in parallel to achieve maximum superposition efficiency. Because of the small beam divergence, very tight tolerances apply to the subtelescope axes' direction. Finally, a near-perfect correspondence between the subfields' states of polarization has to be guaranteed in order to add them coherently and to feed a subsequent coherent receiver. Therefore, the optical components of the phased array have to maintain the state of polarization.

A laboratory demonstrator of a phased telescope array with 16 apertures, to be used in the receive branch of a coherent optical intersatellite link, has been designed, manufactured, and tested at our institute. The work has been done under contract of the European Space Agency (ESA). In the following we describe the phased telescope array's basic principle and introduce our experimental setup. We also present the most important measurement results and compare them with theoretical predictions.

2. BASIC PRINCIPLE

Figure 1 depicts the basic architecture of a phased telescope array comprising only two apertures. The incident plane optical wave (transmitted by an optical point source at very large distance) strikes the subtelescopes' focussing optics. The subfields are shifted in phase by piston actuators and coherently superimposed by an optical beam combiner. Both input ports of the beam combiner carry substantially equal powers. In the desired state of operation, the subfield pistons are always set so that the coherent sum of the input powers appears at the signal output port of the beam combiner(P_A in Figure 1). To achieve this state, the power detected at the beam combiner's control output port, P_B, is minimized by an optical phase locked loop (PLL) employing a dither algorithm. The dither algorithm applies a small periodic piston disturbance and synchronously demodulates the resulting optical power variations. As a consequence, the power/piston characteristic (P_A and P_B as a function of $\phi_1 - \phi_2$) is differentiated, leading to a sinusoidal phase detector characteristic V_{PD}. If the piston control loop is closed, the power at the beam combiner output port is minimized and the total available optical power is directed to the signal output. Hence an automatic tracking of the direction of the incident optical wave is achieved (within an angular range limited only by the diffraction angle of a single subaperture).

Besides setting the subtelescope pistons, the control unit also maintains the relative coalignment of the subtelescope axes. The basic principle of this tilt alignment is to maximize, for each subtelescope, the optical power coupled into the beam combiner. To this end, the piston control loop described above is inverted, causing the power sensor at the control output port of the beam combiner to be fed with the coherent sum of the subtelescope powers. The subtelescopes are then aligned one by one for maximum power at the power sensor. Finally the piston control loop is switched back to normal operation.

The basic phased telescope array architecture shown in Figure 1 can easily be generalized to more than two subapertures by cascading elementary beam combiners to form a binary tree (compare Figure 2). In case the number of subtelescopes is not a power of two, some of the elementary beam combiners have to be asymmetric. We have shown both by experiment[2] and by theoretical analysis[3] that in case of symmetric beam combiners, it is sufficient to employ a single dither frequency for all piston control loops.

3. DEMONSTRATOR DESIGN

The phased telescope array demonstrator has been designed for a wavelength of $\lambda = 1.064\mu m$ and circular input polarization. A block diagram is shown in Figure 2. Sixteen refractive subtelescopes collect the incident optical radiation and couple it into polarization-maintaining single-mode fibers (PMF).

The focussing optics of each subtelescope consists of 3 lenses with a clear aperture diameter of $25mm$. The objectives have a focal length of $92.5mm$ and are manuaftured to diffraction limited quality. All free surfaces are anti-reflection coated at the wavelength of operation. To convert the circular state of polarization of the input field into a linear one required by the optical fiber, each fiber end is equipped with an anti-reflection coated quarter-wave plate.

As tilt actuators we use piezoelectrically driven screws (Model 8351, New Focus, USA). Instead of moving the whole subtelescope (and thus a great amount of mass), the tilt actuators only shift the fiber end in two orthogonal

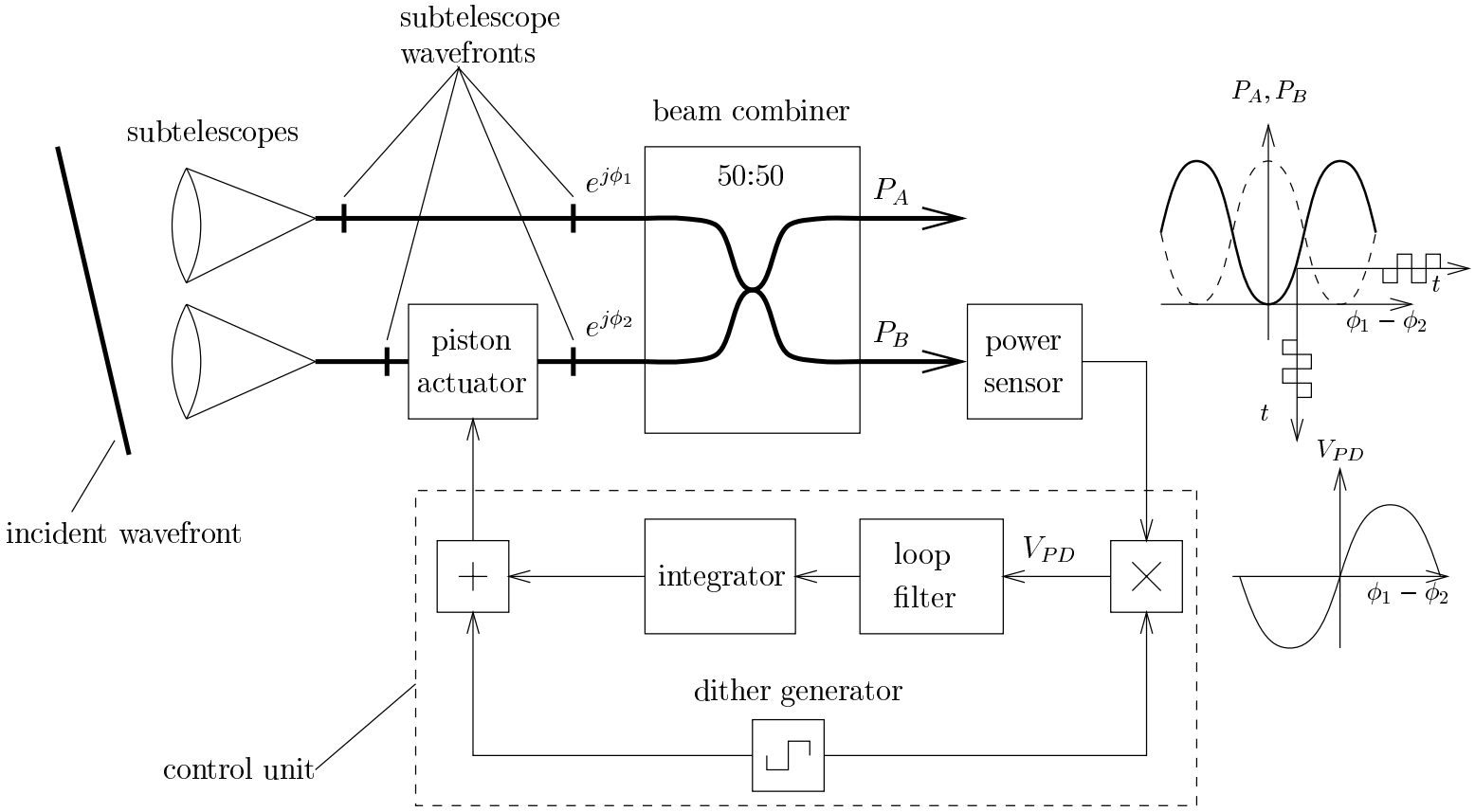

Figure 1. Basic principle of the piston control loop employed in the phased array demonstrator

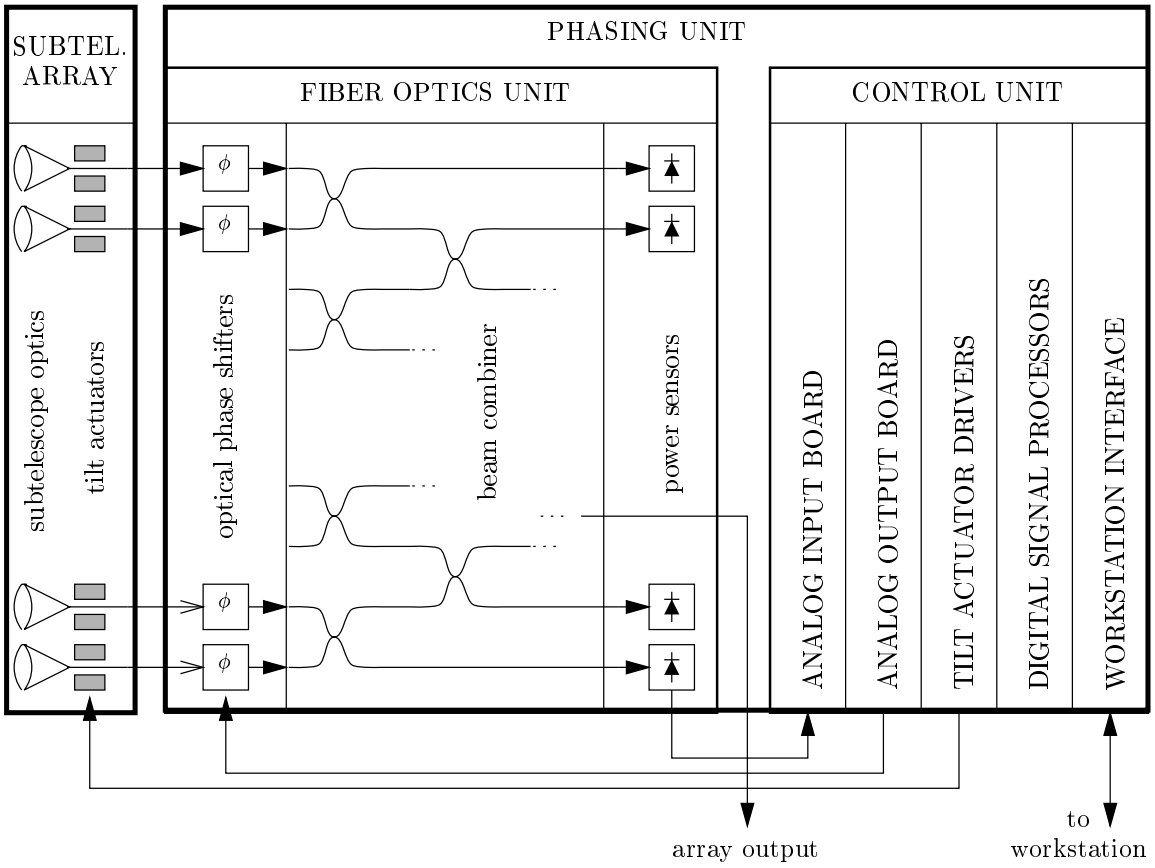

Figure 2. Block diagram of the 16 aperture engineering demonstrator

directions transverse to the telescope axis in the objective's focal plane. The subtelescopes are mounted on a baseplate at a 4×4 Cartesian grid with a mutual distance of $35mm$ (see Figure 3).

The sixteen output fibers of the subtelescope array are connected to the phasing unit shown in Figure 4 via polarization-maintaining fiber connectors.

Fiber stretchers are used as piston actuators. The polarization-maintaining fiber is wrapped around piezoelectric tubes with $14mm$ diameter. By applying a voltage, the diameter of the tube and thus the length of the pertinent fiber is changed.

The beam combiner of the demonstrator is made up of five identical modules each containing three polarization-maintaining fiber directional couplers. To maximize the optical throughput, piston actuators and beam combiner modules are interconnected by fusion splices instead of connectors. One connectorized PMF constitutes the array's optical output.

Fifteen photodetectors sense the power directed to the beam combiners' control output ports. Since optimum phasing is achieved by minimizing the power at these ports, noise introduced by the photodetectors results in piston errors and thus in a reduction of the telescope array's output power. Using InGaAs photodiodes and low noise operational amplifiers we achieved a noise-equivalent input power of some $50nW/\sqrt{Hz}$ and an overall sensitivity of $4 \cdot 10^8 V/W$.

The heart of the phased array's control unit is a dual digital signal processor (DSP) board (Model IXD7232, Ixthos, USA) with VMEbus interface. The DSPs, both ADSP-21020 from Analog Devices operating at $33MHz$, are used for piston control, tilt control, and system testing. Concerning piston control, a dither algorithm with a single dither frequency of $f_d = 20kHz$ is employed. The power sensor output voltages are sampled at a rate of $2 \cdot f_d = 40kHz$. For each set of power samples, the DSP calculates a set of piston actuator values and updates the piston actuators accordingly. We could achieve a very efficient implementation of the dither algorithm: Although

Figure 3. Front view of the demonstrator's subtelescope array

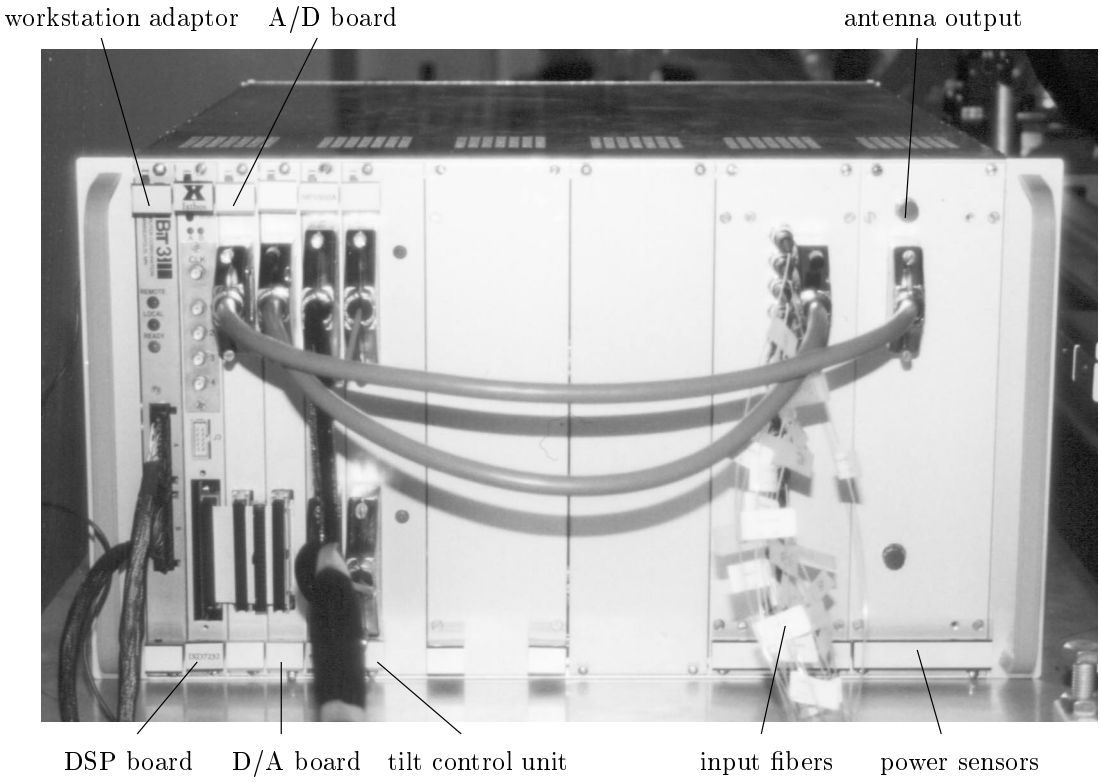

Figure 4. Phasing unit

only 15 control loops are required for a 16 aperture array, a single ADSP-21020 can simultaneously operate up to 63 piston control loops at a sample rate of $2 \cdot f_d = 40kHz$. The second DSP is used for subtelescope tilt alignment and antenna testing.

Custom-built 16-channel analog-to-digital and digital-to-analog converter boards constitute the DSP interface electronics. They are connected to the DSP board via a 32-bit high speed bi-directional bus.

The subsystem driving the tilt actuators consists of two driver circuits (Model 8701, New Focus, USA) and a 32 channel relay board selecting the subtelescope to be aligned. Each of the boards is equipped with a VMEbus interface and is commanded by the DSP board.

For software development, antenna monitoring and testing, the control unit also contains a workstation adaptor (Model 467-1, Bit 3 Corp., USA).

4. TEST SOURCE

In the planned intersatellite link application, the array is illuminated by a laser source at a distance of some $40000km$. The input field hence constitutes a plane, homogeneous wave. In the laboratory we simulate such a uniform plane wave by a fiber-coupled refractive collimator. The 3-lens collimator objective (Spindler&Hoyer, Germany) has a clear-aperture diameter of $194mm$ and a focal length of $900mm$. It is fed by a fiber-coupled Nd:YAG laser with the output fiber end placed in the objective's focal plane. To arrive at the required circular state of polarization, a quarter-wave plate is glued directly to the fiber end. Piezo-electric actuators allow to move the fiber end in the objective's focal plane and thus to tilt the test source beam.

5. MEASUREMENT RESULTS

In this section we summarize the test results obtained with the phased array demonstrator and compare them with the performance predicted by analytical investigation and computer simulation.

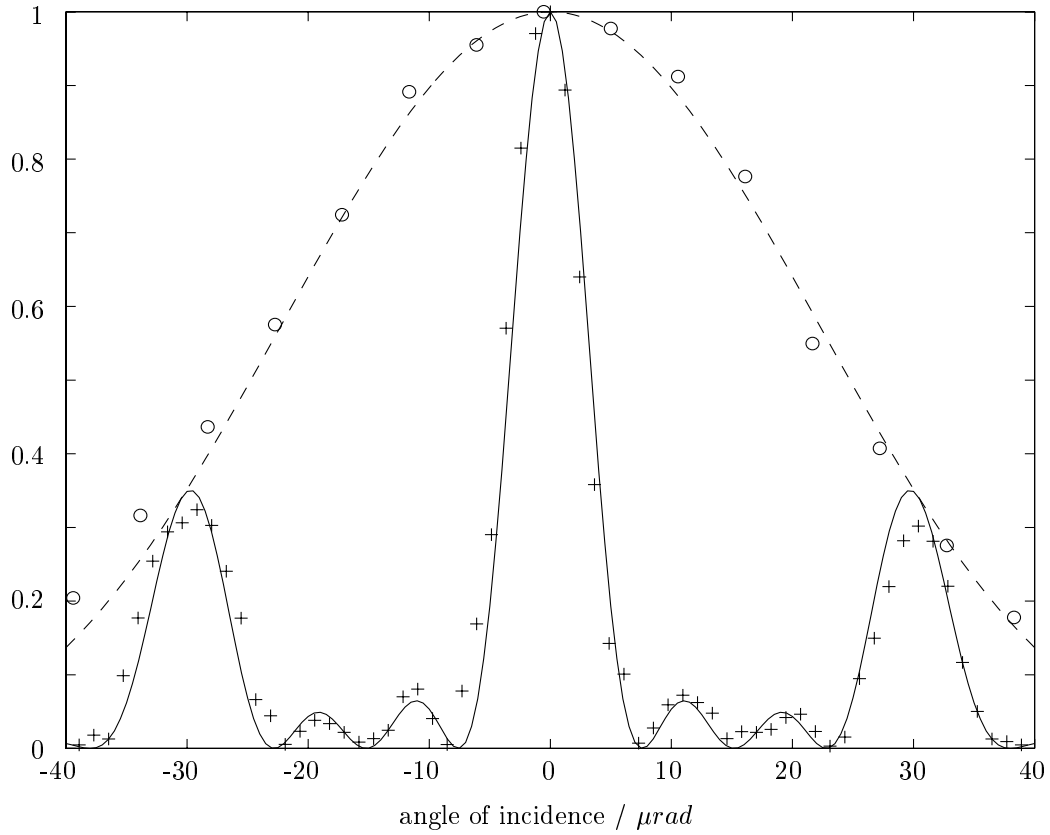

Figure 5. Vertical cross section of the receive characteristic (dashed line ... theory; circles ... measurement), and of the instantaneous array characteristic (solid line ... theory; crosses ... measurement)

Figure 5 shows both theoretical and experimental results of the receive characteristic and the instantaneous array characteristic. The *receive characteristic* is defined as normalized output power versus angle of incidence in case the piston control loops are closed and the angular variations can be compensated by phase control. In theory, it is identical with the characteristic of a single subtelescope. The array's field of view is described by the $-1dB$ tracking angular range, which amounts to $30\mu rad$. The *instantaneous array characteristic* is defined as power versus angle in case the array's mainlobe is fixed, i.e. angular variations of the input field are not compensated by piston control. For both characteristics, very good correspondence between theory and experiment was achieved.

The agility of the array's adaptive tracking has been tested by adding sinusoidal error signals to the signals driving the piston actuators and measuring the resulting piston variations in closed-loop operation as a function of frequency. We chose this method instead of deflecting the test source beam and measuring the mainlobe axis variation because of the limited agility and the nonlinearity of the test source's piezo-electric actuators. Figure 6 depicts the tracking error response, i.e. the factor by which a small angular disturbance is suppressed, as a function of frequency. The $-3dB$ tracking error bandwidth amounts to $730Hz$. Hence, the automatic fine tracking mechanism covers the typical range of satellite vibrations extending up to a few hundred Hertz.

As already mentioned in Section 3, noise occuring within the piston control loops reduces the the array's superposition efficiency and thus the total output power. Figure 7 shows the phasing efficiency, i.e. the mean output power reduction factor due to noise in the piston control loops, as a function of the optical input power level. It remains above 99% for input powers as low as $50nW$.

The output power available to a subsequent coherent receiver is further reduced by polarization crosstalk, since the output field has to be superimposed with the receiver's local oscillator. By careful selection and assembly of the optical components we achieved a near-perfect linear state of polarization at the array's output interface. The average polarization extinction ratio amounts to $24dB$.

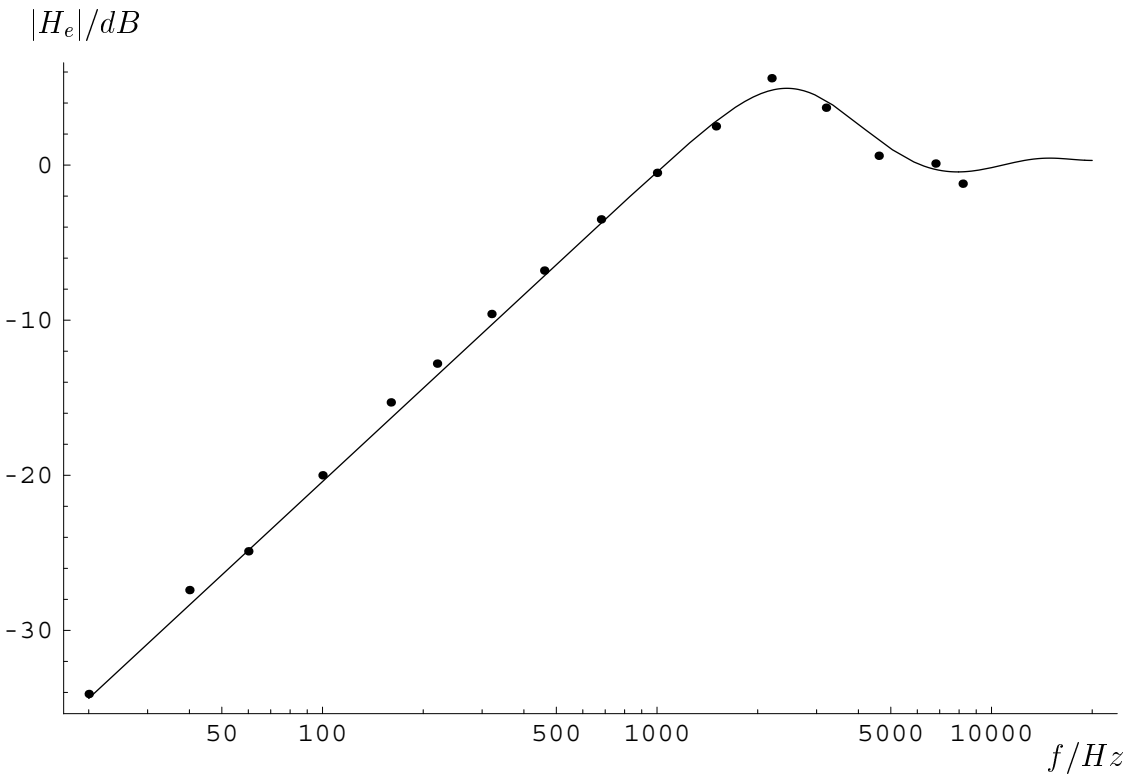

Figure 6. Calculated (solid line) and measured (dots) tracking error response of the phased array demonstrator

Despite the high phasing efficiency and the excellent output state of polarization, the phased array's overall optical throughput (i.e. the ratio of the power available at the array's output fiber and the total incident power at the subtelescopes' entrance pupils) amounts only to $-11.8dB$. The low value is mainly caused by the fiber-optic beam combiner (approximately $8dB$ loss). Therefore, we are currently investigating alternative beam combiner realizations promising an overall throughput on the order of $-3.5 \ldots -4.5dB$.

We successfully demonstrated data transmission via the phased array antenna at a data rate of $565Mbit/s$. The data was phase modulated upon the optical carrier and detected by a coherent optical receiver.

6. CONCLUSION

The engineering demonstrator of a phased receive telescope array for coherent space communications has been realized and tested. The experimental results show good correspondence with the predicted performance and encourage the design and realization of an operational array to be tested in free-space environment. The concept will further benefit from new developments in the emerging field of integrated optics.

ACKNOWLEDGMENTS

The contents of this paper evolved from a research project supported by the European Space Agency. We thank Bernhard Furch for supervising and promoting this work.

REFERENCES

1. V. W. S. Chan, "Space coherent optical communication systems — an introduction," *IEEE Journal of Lightwave Technology* **5**(4), pp. 633–637, 1987.
2. K. H. Kudielka *et al.*, "Experimental verification of an adaptive optical multi-aperture receive antenna for laser space communications," in *Proc. SPIE*, vol. 2123, pp. 478–486, 1994.
3. K. H. Kudielka *et al.*, "Adaptive optical multi-aperture receive antenna for coherent intersatellite communications," in *Proc. SPIE*, vol. 2210, pp. 61–70, 1994.

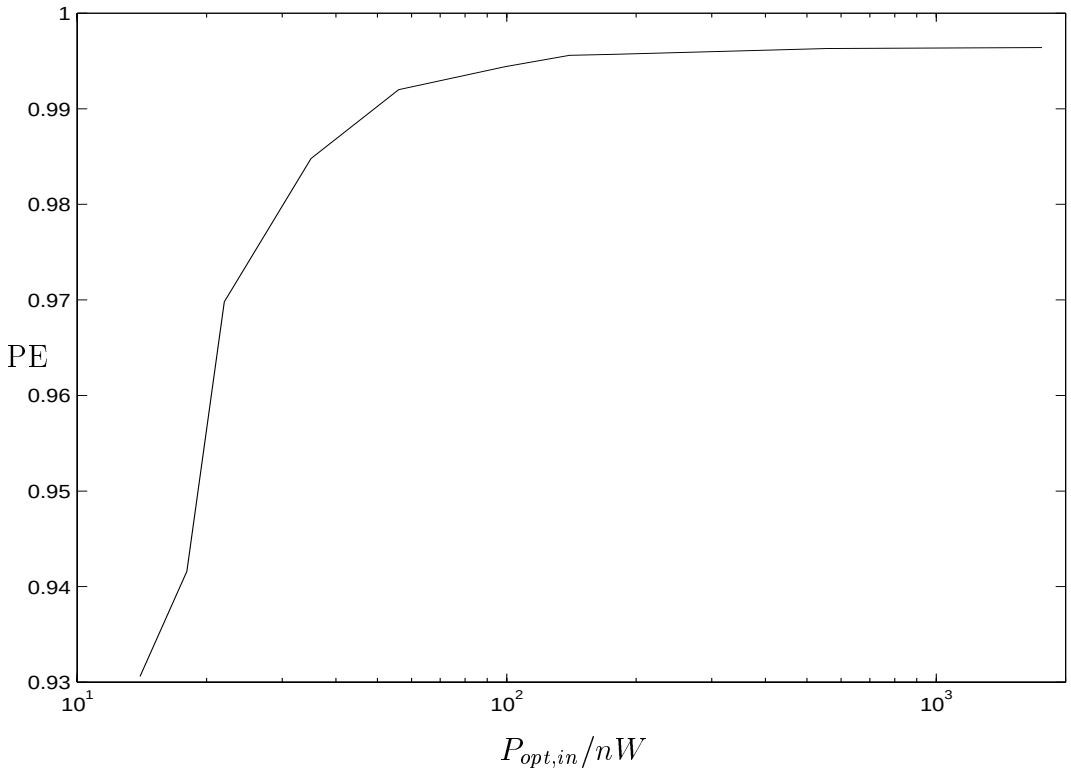

Figure 7. Phasing efficiency as a function of total incident power